III International Conference on Particle-based Methods – Fundamentals and Applications
PARTICLES 2013
M. Bischoff, E. Oñate, D.R.J. Owen, E. Ramm & P. Wriggers (Eds)

COMPARISON OF COUPLED DEM-CFD AND SPH-DEM METHODS IN SINGLE AND MULTIPLE PARTICLE SEDIMENTATION TEST CASES

Mohammadreza Ebrahimi[1], Prashant Gupta[1], Martin Robinson[2], Martin Crapper[1], Marco Ramaioli[3], Jin Y. Ooi[1]

[1]School of Engineering, The University of Edinburgh,
The King's Buildings, Edinburgh EH9 3JL, UK
M.Ebrahimi@ed.ac.uk

[2]Mathematical Institute, University of Oxford
24-29 St Giles, Oxford OX1 3LB, UK
Martin.Robinson@maths.ox.ac.uk

[3]Nestlé Research Centre, Lausanne, Switzerland
Marco.Ramaioli@rdls.nestle.com

Keywords: DEM-CFD, DEM-SPH, Multiphase flow, particle sedimentation

Summary: *In this paper, the capability of two major methods for modelling two-phase flow systems, coupled discrete element method and computational fluid dynamics (DEM-CFD) and smoothed particle hydrodynamics and discrete element method (SPH-DEM), is investigated. The particle phase is modelled using the discrete element method DEM, while the fluid phase is described using either a mesh-based (CFD) or a mesh-less (SPH) method. Comparisons are performed to address algorithmic differences between these methods using a series of verification test cases, prior to its application to more complex systems. The present study describes a comprehensive verification for the fluid-particle simulations with -two different test cases: single particle sedimentation and sedimentation of a constant porosity block. In each case the simulation results are compared with the corresponding analytical solutions showing a good agreement in each case.*

1 INTRODUCTION

A wide range of industrial processes involves multiphase granular flows, for example catalytic cracking in fluidized beds, pneumatic conveying of raw materials and gas-particle separation in a cyclone. Knowledge of the underlying physics of fluid-solid and inter-particle phenomena is limited due to wide separation of scales in time and space. Pilot scale experiments are limited, time consuming and expensive. With the advent of increased computational power, fluid-particle flows for different regimes (dilute or dense) can be modelled with a multi-phase modelling strategy [1]. Which strategy employed is mostly a

trade-off between the desired level of modelling detail and computational expense. Hybrid schemes are closed by constitutive modelling through micro-mechanical parameterization [2]. Commonly used models employed in literature to model laboratory scale experiments are: the two-fluid modelling (TFM), coupled DEM-CFD [3] and coupled SPH-DEM modeling [4]. Significant challenges remain, notably in appropriate definition of boundary conditions, constitutive micro-mechanical modelling and establishing relative significance of effects such as drag, lift forces and turbulence, and the availability of model verification and validation test cases.

TFM treats the solid and gas phases as interpenetrating continua, exchanging momentum [1]. These models are computationally inexpensive, but particle level interactions cannot be captured and accuracy of the simulations is severely compromised [5]. Direct numerical simulation (DNS) can be employed to study particle-particle and particle-fluid interaction (e.g. Lattice Boltzmann simulations), but are so computationally expensive that even simulation of laboratory scale experiments is not feasible. Nevertheless, these simulations provide a route to micro-mechanical constitutive modelling to put at continuum scale, as extensively reviewed in [1]. Lagrangian models can be employed to describe the particle phase in conjunction with an Eulerian framework to model the fluid phase, an example of this being DEM-CFD modelling. In this approach, the governing equations for the fluid motion are averaged, and each particle's motion is separately tracked. This avoids the DNS of fluid motion and can capture particle dynamics more accurately than any continuum description of solid phase[2,6,7].

SPH-DEM is a purely particle-based solution method modelled in a Lagrangian framework. Rather than using a fixed grid, the Smoothed Particle Hydrodynamics method models the fluid using an unstructured set of points that move with the fluid velocity [8]. The fluid variables and their spatial gradients are interpolated between these points using a Gaussian-like radial smoothing kernel. This is coupled with a DEM model for the solid phase, avoiding the need for a computational mesh entirely. A brief outline of key differences between SPH-DEM and DEM-CFD is as shown in Table 1. The difference between the mesh/grid based and SPH methods leads to different scenarios, where each of the methods can be advantageous over the other. The main advantage of SPH over the grid-based methods is its adaptability during time-evolving dynamic processes in time and space [8]. The lack of mesh is advantageous in applications where the continual updating of mesh connectivity presents a difficult problem, such as free surface flow or the flow around complicated or intermeshing moving boundaries. In these cases the mesh can deform considerably or even change topology entirely, but a particle-based method such as SPH is unaffected. However, SPH can be affected by particle disorder and suffers from poor accuracy of spatial gradients. DEM-CFD is a well-established mesh based method to model fluid-particle interactions. CFD has been studied for decades and has a large literature for mesh discretization schemes and solutions. Computationally, SPH is more expensive than CFD. However, since the work is in a coupled framework, the computational load is normally determined by the DEM, depending on how dilute or dense the system is.

Table 1: Comparison SPH-DEM and DEM-CFD

	SPH-DEM	**DEM-CFD**
Fluid model	Lagrangian frame: fluid discretized to mass "particles" moving with local fluid velocities	Eulerian model
Discretization of domain	No mesh. Fluid variables interpolated between points using a radial smoothing kernel function	Mesh is decided on the basis of convergence of fluid field and minimum number of particles in a fluid cell for averaging statistics
Information tracking	Information stored based on the particle movement	Porosity, momentum and pressure information is based on the fluid cell centre or the cell faces
Averaging of fluid variables	Averaged Navier-Stokes (NS) equations are interpolated over each particle and its nearest neighbors using SPH smoothing kernel	NS equations are coarse-grained to include particle-level information from DEM at a continuum scale

Careful verification and validation (V&V) is required before implementing model codes to study physical processes. Verification can be referred to as the process of determining whether the computational model represents the underlying mathematical model and its solutions. Validation can be referred to as the process of determining the degree to which the model as applied is an accurate representation of the real world. When analytical solutions are available, these two aspects can converge. In this work, test cases are used to verify that codes correctly model the dynamics of two-phase flows and the interaction between phases. Two sedimentation test cases are studied here: single particle sedimentation (SPS) and a constant porosity block (CPB). The degree of complexity of these test cases increases from the first example to the second. Single particle sedimentation checks the drag force implementation (calculation and integration) for a single particle falling through different fluid media. These results can be compared to creeping flow single particle approximations in the Stokesian regime. The CPB checks the drag model implementation for both phases for a constant porosity field and a simple velocity field. The main objectives of this study are to compare between the SPH-DEM and DEM-CFD and to establish the level of discrepancy between these numerical methods and the corresponding analytical solutions.

2 EQUATIONS OF MOTIONS

2.1 DEM-CFD

DEM-CFD methods are based on the locally averaged Navier-Stokes equations [9] coupled with a Lagrangian framework to track the motion of each particle by solving Newton's second law of motion in a two-way coupling approach [2,6]. The DEM-CFD simulations were performed with an in-house built coupled OpenFOAM and LAMMPS code [10] and also the commercial EDEM-FLUENT code. The SPH-DEM simulations were performed using an in-house code which has been previously shown to produce good results for two test cases [4]. In each method, the fluid phase is described by the conservation equations of mass and momentum. Newton's second law of motion tracks translational and rotational motion of the particles:

$$\frac{\partial(\varepsilon\rho_g)}{\partial t} + \left(\nabla.\varepsilon\rho_g u\right) = 0 \tag{1}$$

$$\frac{\partial(\varepsilon\rho_g)}{\partial t} + \left(\nabla.\varepsilon\rho_g u\right) = -\varepsilon\nabla p + S_p - \nabla.(\varepsilon\overline{\tau}) + \varepsilon\rho g \tag{2}$$

$\varepsilon, \rho_g, u, \overline{\tau}$ and p are the porosity, density, velocity, viscous stress tensor and the pressure of the gas phase respectively. For DEM-CFD, the momentum source term is defined as

$$S_p = \frac{1}{V}\int \sum_{a=0}^{N_{part}} \frac{\beta V_a}{1-\varepsilon}(u - V_a)\delta(r - r_a)dV \tag{3}$$

The interphase momentum exchange can be modelled by drag force. β is the drag law coefficient.

2.2 SPH-DEM

Here we briefly describe the governing equations for SPH-DEM, based on the locally averaged Navier-Stokes equations (LANSEs) derived by Anderson and Jackson [9] and given in equations (4) and (5). For more details on SPH-DEM please see Robinson et al. [4]. We define a smooth porosity field by smoothing out the DEM particle's volumes according to the SPH interpolation kernel $W_{aj}(h) = W(r_a - r_j, h)$

$$\varepsilon_a = 1 - \sum_j W_{aj}(h)V_j \tag{4}$$

where V_j is the volume of DEM particle *j*. For readability, sums over SPH particles use the subscript *b*, while sums over surrounding DEM particles use the subscript *j*. To calculate the continuity and momentum equations in the LANSEs, we first define a superficial fluid density ρ equal to the intrinsic fluid density scaled by the local porosity $\rho = \varepsilon\rho_f$. Substituting the superficial fluid density into the averaged continuity and momentum equations reduces them to the normal Navier-Stokes equations. The approach of SPH-DEM is therefore to use the weakly compressible SPH equations with variable *h* (resolution/smoothing length) terms and adding fluid-particle coupling terms (as specified below).The rate of change of superficial density for each SPH particle *a* is given by

$$\frac{D\rho_a}{Dt} = \frac{1}{\Omega_a}\sum_b m_b \boldsymbol{u}_{ab} \cdot \triangle_a W_{ab}(h_a) \tag{5}$$

$$\Omega_a = 1 - \frac{\partial h_a}{\partial \rho_a}\sum_b m_b \frac{\partial W_{ab}(h_a)}{\partial h_a} \tag{6}$$

The SPH acceleration equation is given by

$$\frac{D\boldsymbol{u}_a}{Dt} = -\sum_b \left(\frac{P_a}{\Omega_a\rho_a^2} + \Pi_{ab}\right) \triangle_a W_{ab}(h_a) + \left(\frac{P_b}{\Omega_b\rho_b^2} + \Pi_{ab}\right) \triangle_a W_{ab}(h_b) + \frac{\boldsymbol{f}_a}{m_a} \tag{7}$$

Where the Π_{ab} models the viscous term and P_a is the pressure from the equation of state (see below). $\boldsymbol{f}_a$ is the coupling force on the SPH particle *a* due to the DEM particles. The coupling force on SPH particle *a* is determined by a weighted average of the fluid-particle coupling forces on the surrounding DEM particles.

$$\boldsymbol{f}_a = \frac{m_a}{\rho_a}\sum_j \frac{1}{S_j}\boldsymbol{f}_j W_{aj}(h_a) \tag{8}$$

$\boldsymbol{f}_j$ is the fluid-particle coupling force calculated for each DEM particle (given by the last two terms in equation (8)) and $S_j = \sum_b \frac{m_b}{\rho_b} W_{jb}(h_b)$ is a correction factor to guarantee equal and opposite forces between the two phases. The fluid pressure P_a is calculated using the weakly compressible equation of state where the reference density ρ_0 is scaled by the local porosity to ensure that the pressure is slowly varying with porosity as:

$$P_a = B\left(\left(\frac{\rho_a}{\varepsilon_a \rho_0}\right)^{\gamma} - 1\right) \tag{9}$$

The smoothing length h_a varies according to the superficial density (and hence with the porosity) and is calculated by $h_a = 1.5(m_a/\rho_a)^{1/3}$.

2.3 Drag models

This section describes briefly how fluid-particle interactions described in sections 2.1 and 2.2 are implemented. In general, drag force on a particle in a multiple particle domain is given in all *Re*-number regimes as

$$F_{drag} = \frac{1}{8} C_d f(\varepsilon_i) \pi d^2 \rho_f |u_t| u_t \tag{10}$$

$$u_t = \varepsilon(v_p - v_f) \tag{11}$$

Where C_d is the drag coefficient which varies with the particle Reynolds number $Re = \rho_f |u_t| d/\mu$ and $f(\varepsilon_i)$ is the voidage function [11] ; $v_p - v_f$ is the velocity difference between the particle and fluid phases . For a single sedimenting particle, the voidage function can be taken as $f = 1$. For the DEM-CFD drag model [12] C_d is defined as follows:

$$C_d = \begin{cases} \dfrac{24}{Re} & Re < 0.5 \\ \dfrac{24}{Re}(1.0 + 0.15Re^{0.687}) & 0.5 \leq Re < 1000 \end{cases} \tag{12}$$

The SPH-DEM Stokes drag is similar but without the *Re* number dependence for higher *Re* > 0.5. For higher Re numbers and multiple particle, the Di Felice drag model can be used [11].

$$C_d = [0.63 + 4.8/\sqrt{Re}]^2 \tag{13}$$

$$f(\varepsilon_i) = \varepsilon_i^{-\xi} \tag{14}$$

$$\xi = 3.7 - 0.65exp\left[-\frac{(1.5 - log_{10}Re)^2}{2}\right] \tag{15}$$

Another drag model used in this study which is valid for high *Re* number, was proposed by Coulson-Richardson [13].

$$f_d = \frac{\pi}{4} d^2 \rho_f |u_t| (1.8Re^{-0.31} + 0.293Re^{-0.06})^{3.45} \tag{16}$$

β (drag model coefficient in equation (3)) as mentioned in Section 2 can be related to C_d through simple mathematical algebraic manipulations as done in [10]. These drag models are used in SPS or CPB studies according to the applicability. Implementation of drag models for DEM-CFD and SPH-DEM can be studied from [4,10].

2.4 DEM

The solid phase motion is described using a DEM approach to solve Newton's 2nd Law of Motion [14]:

$$m\frac{d^2r}{dt^2} = F_{contact} + mg + \frac{\beta V_a}{1-\varepsilon}(u - V_a) - V\nabla p \qquad (17)$$

$F_{contact}$ is the contact force modelled as a linear spring-dashpot model [14]. The coefficient of restitution (e) provides a route of energy dissipation due to collisions. The last two terms describe the coupling force on each DEM particle due to the fluid.

3 SIMULATION SET-UP

The simulation domain and solid particle properties are shown in Table 2. The domain comprises a column under gravity (negative z direction) with a no-slip boundary condition at the bottom and periodic boundary conditions elsewhere.

Table 2: Simulation domain and particle properties

Parameters	Value
Box width (m)	4e-3
Box height (m)	6e-3
Particle diameter (m)	1e-4
Particle density (kg/m^3)	2500

The fluid-particle relaxation time is shown in Table 3, which provides a timescale for the fluid-particle interaction forces. The time-step for the fluid phase is set to an order of magnitude lower than the relaxation time. The particle Reynolds number is defined using the superficial velocity (relative velocity of particle with respect to surrounding fluid divided by porosity) and the diameter of the particle as a characteristic length. The CPB is created using a regular grid of DEM particles that are separated by a constant $\Delta r = (V/1-\varepsilon)^{1/3}$ (V is the particle volume and ε is the porosity of the case). The DEM particle positions are fixed relative to each other during the simulation. To implement this for the CPB tests, the drag force calculated for each particle is summed over the CPB and then divided equally among all its component particles, thus ensuring each particle experiences an equal drag force. For the CFD simulation of the CPB, the fluid mesh is created with respect to the distance between the particles, giving 8 particles in each fluid cell, placed symmetrically. This means that each particle would 'experience' equal porosity except for the boundary particles which would

experience a reduced porosity than the rest of the block at certain times (hence the need for averaging the drag force over all particles).

Table 3: Fluid properties

Parameters	Air	Water	Water-Glycerol
Fluid density (kg/m^3)	1.1839	1000	1150
Fluid viscosity (Pa.s)	1.86e-5	8.9e-4	8.9e-3
Porosity		0.6-1	
Calculated terminal velocity (m/s)	0.0102-0.5	1.3-7.6e-3	1.3-8.4e-4
Fluid CFL conditions (s)		1.4-4.5e-5	
Particle Reynolds number	0.65-3.19	0.15-0.85	0.002-0.011
Relaxation time (s)	7.47e-2	1.56e-3	1.56e-4

4 SIMULATION RESULTS

4.1 Single particle sedimentation (SPS)

This section describes comparison of results from SPH-DEM and DEM-CFD for SPS. Different fluid properties and drag models are tested. In the Stokesian or creeping flow regime (Re < 0.5), the following analytical equation can be solved to calculate the terminal velocity:

$$v(t) = \frac{(\rho_{p-}\rho)Vg}{b}(1 - e^{-bt/m}) \tag{18}$$

$$b = 3\pi\mu d \tag{19}$$

Here μ is the dynamic viscosity of the fluid, d is the diameter of the particle, V is the particle volume and $\rho_p - \rho$ denotes the density difference between solid and fluid media. Figure 1 gives the DEM-CFD and SPH-DEM results for single particle sedimentation in air, water and a water- glycerol solution using the Stokes drag model. Both SPH-DEM and DEM-CFD results for terminal velocity are within 1% error for water-glycerol, 3% error for water and 5% for air. These results show the terminal velocity dependence on Re number (when greater than 0.5). In Figure 2, the Di Felice drag model (in the limiting condition of ($\varepsilon_i \rightarrow 1$) and Coulson-Richardson drag model [13] are implemented to compare against the Stokes drag model. Fully resolved COMSOL Multiphysics (finite element analysis, solver and simulation software http://www.comsol.com/) is used for a reference terminal velocity in this study. Figure 2(a) shows the SPH-DEM terminal velocity % errors with Re number up to 10 using the three different drag forces. For SPH-DEM, the results for the various drag models differ

in their prediction by 6% for single particle sedimentation in water (except for Stokes drag, which diverges for larger *Re* due to the assumption of creeping flow). In contrast, the Stokes drag for the DEM-CFD simulations (Figure 2(b)) has an *Re* dependence for *Re* > 0.5 and is thus comparable to the fully resolved COMSOL results.) The Coulson-Richardson drag force gives the closest results to the reference terminal velocity.

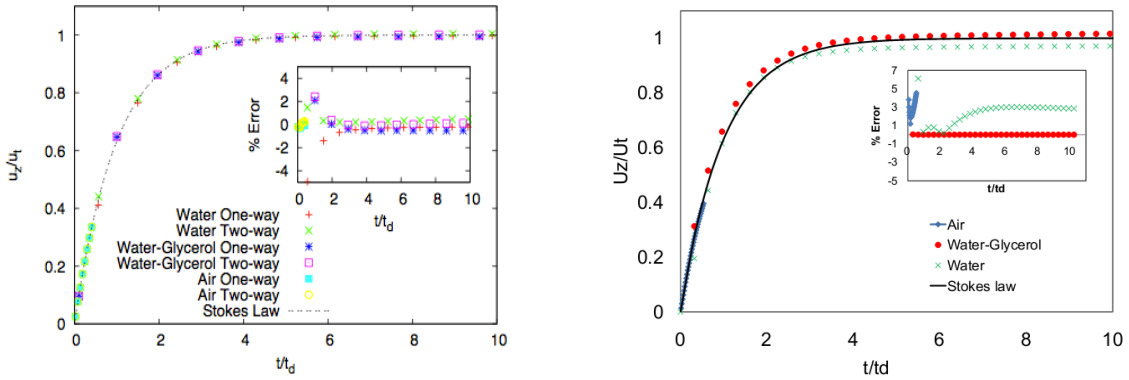

(a) (b)

Figure 1: (a) Normalized terminal velocity for SPH with different media and coupling (one-ways mean fluid is not affected by particle motion). (b) Normalized terminal velocity for SPS using DEM-CFD in different medium.

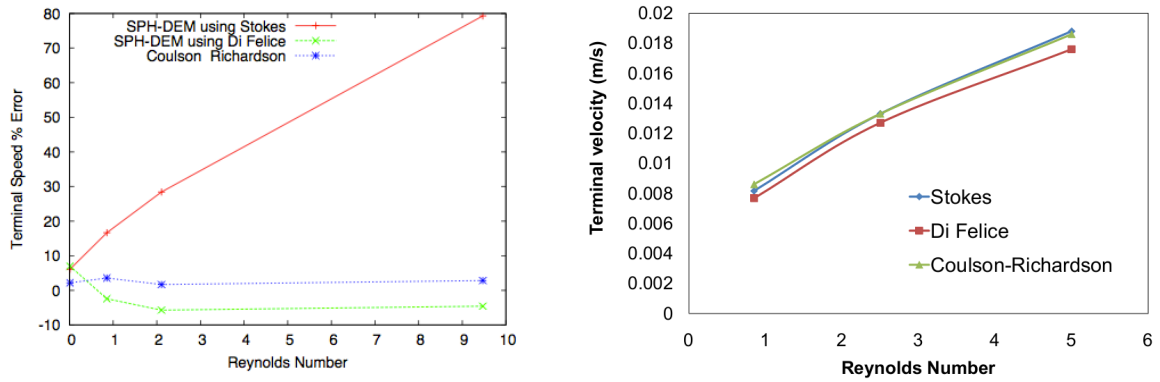

(a) (b)

Figure 2: (a) Error in SPH-DEM average SPS terminal velocity at different *Re* number with against COMSOL fully resolved simulation used as reference (b) DEM-CFD results for terminal velocity vs *Re* number for different drag models.

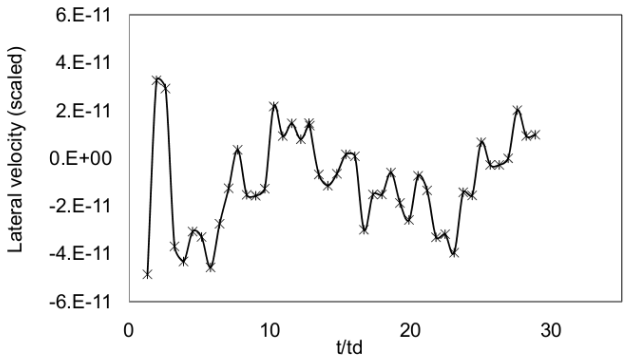

Figure 3: DEM-CFD results for the small fluctuating numerical error in the lateral velocity due to buoyancy and drag calculations.

In Figure 3, DEM-CFD shows a lateral velocity (magnitude 1e-11) which can be attributed to the numerical errors due to discretization schemes. These errors come primarily from the buoyancy calculations (pressure calculations updated only at the fluid step). Numerical errors are fluctuating and do not accumulate with time. For SPH-DEM, the smoothing length h dictates the fluid resolution as opposed to mesh size in DEM-CFD. DEM-CFD calculates porosity based on the mesh cell volume, hence predicts lower porosity for finer mesh size. This can lead to unphysical low porosity even for a single particle in the domain. Usual DEM-CFD methodology states that the minimum cell size should be sufficiently larger than the largest DEM particle diameter in order to reduce these unphysical porosities [9]. SPH-DEM results in [4] indicate that the fluid resolution (i.e. the smoothing length h) should be kept greater than two times the DEM particle diameter.

4.2 Constant Porosity Block (CPB)

The second test case models the sedimentation of the CPB in water. The simulation domain is otherwise identical to the SPS test case. Using the Di Felice drag equation, the expected terminal velocity of the block is calculated by the following equation, based on the particle Re number

$$0.392Re^2 + 6.048Re^{1.5} + 23.04Re - 1.333Ar\varepsilon^{1+\xi} = 0 \qquad (20)$$

Where $Ar = d^3\rho(\rho_p - \rho)g/\mu^2$ is the Archimedes number. Figure 4 shows the scaled average terminal velocity plotted with respect to porosity. High porosity cases tend to have lower error compared with low porosity cases. This trend can be explained by the fact that analytical solution does not consider the effects of interstitial fluid velocity and the porosity is assumed to be constant throughout the block (the DEM particles at the edge of the block experience a lower porosity). Figure 5 shows the % error in terminal velocity calculated using

different time step ratios in DEM-CFD (the fluid time-step was changed while keeping the DEM time-step constant) it can be seen from these results that a lower time-step ratios tend to improve the fluctuations in the results. Lowering CFD time step increases the computational time considerably but does not improve numerical results significantly.

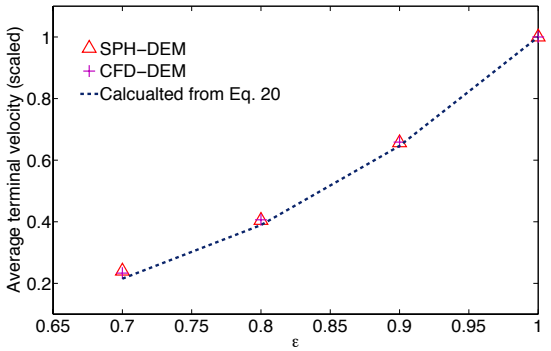

Figure 4: Average terminal velocity (scaled by the expected terminal velocity of single particle calculated by equation 20) for CPB: SPH-DEM and DEM-CFD in water, for varying porosities

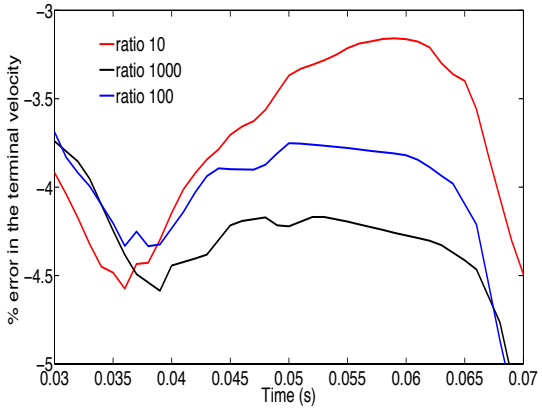

Figure 5: Errors due to differences in fluid and particle time steps in DEM-CFD, depends upon particle relaxation times

5 CONCLUSION

SPH-DEM and DEM-CFD have been presented as tools to simulate fluid-particle coupled systems. Locally averaged Navier-Stokes equations are coupled with discrete element method (DEM) through momentum exchange terms. SPH-DEM and DEM-CFD can be contrasted to give the effects of meshless and mesh dependent methods.

- For single particle sedimentation in air, water and water-glycerol, both the methods give reasonable errors of 1-5 % from analytical solutions (solving the Stokes equation

under creeping flow conditions). However, it must be noted that the $Re < 0.5$ condition was violated in cases with air and water. Fluid resolution effects vary in different ways between the two modelling techniques.

- Mesh effects can be seen more prominently in DEM-CFD as the porosity and momentum exchange terms are calculated based on the mesh. There is a small fluctuating lateral velocity in the DEM-CFD results that does not affect the long term simulation (fluctuations average to zero). The effect of fluid to particle time-step ratio can be seen on single particle sedimentation in DEM-CFD simulation; a lower ratio ensures better coupling and information exchange between 2 phases, although computational costs are higher.

- Multiple particle sedimentation was tested using the sedimentation of a constant porosity block over porosity ranges 0.6-0.9, and *Re* 0.002 to 0.85. Results were close and error limited to 8% in the worst case for DEM-CFD and 5% for SPH-DEM. Error contributions for DEM-CFD were attributed to the mesh size and fluid-particle time step.

- SPH-DEM suffered with inability to resolve the porosity field near the edge of the block, resulting in a reduced porosity field in this region, however DEM-CFD calculated the porosity in the cell as per the volume contribution by particle, which is more accurate than the SPH-DEM. High porosity gradients give rise to fluctuations in SPH fluid velocity leading further to fluctuations in the pressure field (leading to numerical error in the buoyancy force calculations). DEM-CFD counters these issues, as the porosity is calculated exactly with respect to the particle contribution to that fluid cell.

In summary, both SPH-DEM and DEM-CFD simulations were in good agreement with the analytical equations for the two test cases. However, a challenge remaining in improving SPH-DEM is the resolution of high porosity gradients. Promising results have been obtained by calculating the drag separately on the fluid or re-deriving the SPH equations from Lagrangian formulation. For DEM-CFD, challenges remain concerning the influence of mesh size on the particle-fluid dynamic system. Optimisation of fluid mesh size with respect to statistics and the fluid field solution is an important consideration.

6 ACKNOWLEDGMENTS

This work is supported by PARDEM (www.pardem.eu) collaboration, which is a EU Funded Framework 7, Marie Curie Initial Training Network.

7 REFERENCES

[1] M.A. der Hoef, M. van Sint Annaland, N.G. Deen, J.A.M. Kuipers, Numerical simulation of dense gas-solid fluidized beds: A multiscale modeling strategy, Annu. Rev. Fluid Mech. 40 (2008) 47–70.

[2] Y. Tsuji, T. Kawaguchi, T. Tanaka, Discrete particle simulation of two-dimensional fluidized bed, Powder Technology. 77 (1993) 79–87.

[3] J.A.M. Kuipers, W.P.M. Van Swaaij, Computational fluid dynamics applied to chemical reaction engineering, Advances in Chemical Engineering. 24 (1998) 227–328.

[4] M. Robinson, S. Luding, M. Ramaioli, Fluid-particle flow modelling and validation using two-way-coupled mesoscale SPH-DEM, arXiv Preprint arXiv:1301.0752. (2013).

[5] J. Wang, M.A. der Hoef, J.A.M. Kuipers, Why the two-fluid model fails to predict the bed expansion characteristics of Geldart A particles in gas-fluidized beds: a tentative answer, Chemical Engineering Science. 64 (2009) 622–625.

[6] B.H. Xu, A.B. Yu, Numerical simulation of the gas-solid flow in a fluidized bed by combining discrete particle method with computational fluid dynamics, Chemical Engineering Science. 52 (1997) 2785–2809.

[7] K.D. Kafui, C. Thornton, M.J. Adams, Discrete particle-continuum fluid modelling of gas--solid fluidised beds, Chemical Engineering Science. 57 (2002) 2395–2410.

[8] J.J. Monaghan, Smoothed particle hydrodynamics, Reports on Progress in Physics. 68 (2005) 1703.

[9] T.B. Anderson, R. Jackson, Fluid mechanical description of fluidized beds. Equations of motion, Industrial & Engineering Chemistry Fundamentals. 6 (1967) 527–539.

[10] H. Xiao, J. Sun, Algorithms in a Robust Hybrid CFD-DEM Solver for Particle-Laden Flows., Communications in Computational Physics. 9 (2011) 297.

[11] R. Di Felice, The voidage function for fluid-particle interaction systems, International Journal of Multiphase Flow. 20 (1994) 153–159.

[12] R. Clift, J.R. Grace, M.E. Weber, 1978, Bubbles, Drops, and Particles. Academic Press, New York, (n.d.).

[13] J.M. Coulson, J.F. Richardson, D.G. Peacock, Coulson & Richardson's Chemical Engineering: Chemical & biochemical reactors & process control, Elsevier, 1994.

[14] P.A. Cundall, O.D.L. Strack, A discrete numerical model for granular assemblies, Geotechnique. 29 (1979) 47–65.